Meson Spectra from a Dynamical Three-Field Model of AdS/QCD

A THESIS
SUBMITTED TO THE FACULTY OF THE GRADUATE SCHOOL
OF THE UNIVERSITY OF MINNESOTA
BY

Sean Peter Bartz

IN PARTIAL FULFILLMENT OF THE REQUIREMENTS
FOR THE DEGREE OF
DOCTOR OF PHILOSOPHY

Joseph I. Kapusta

August, 2014

Acknowledgements

There are many people that have earned my gratitude for their contribution to my time in graduate school.

This research is supported by the Department of Energy Office of Science Graduate Fellowship Pro- gram (DOE SCGF), made possible in part by the American Recovery and Reinvestment Act of 2009, administered by ORISE-ORAU under contract no. DE-AC05-06OR23100, by the US De- partment of Energy (DOE) under Grant No. DE-FG02-87ER40328, and by a Doctoral Dissertation Fellowship from the University of Minnesota.

Dedication

To my parents, Larry and Colleen, my first teachers. To my sister, Haley, my first student. To my wife, Alicia, my greatest support.

Abstract

Gauge/gravity dualities are a tool that allow the analytic analysis of strongly-coupled gauge theories. The Anti-de Sitter Space/Conformal Field Theory conjecture posits a duality between ten-dimensional string theory and a super Yang-Mills theory. A phenomenologically-motivated modification of this correspondence is known as AdS/QCD, a duality between strongly-coupled QCD-like theories and weakly-coupled gravitational theories in an additional dimension. QCD is not scale-invariant, so the dual theory must be modified in the conformal dimension to reflect this.

This thesis examines "soft-wall" models of AdS/QCD, wherein the conformal symmetry is broken by a field known as a dilaton. The dynamics of the dilaton and other background fields are examined, and a potential for these fields is determined. The background fields are numerically derived from this potential and used in the calculation of meson spectra, which match well to experiment.

The work presented here is based upon previously-published work by the author:

Contents

List of Tables

List of Figures

Chapter 1

Introduction

- Chapter 2 briefly presents the history of, and science behind, the subjects presented in this thesis.
- In Chapter 3 the experiment is outlined.
- Chapter 4 describes the simulation process used in the analysis.
- Chapter 5 follows the chain of reconstruction software used to obtain meaningful results from data.
- Chapter 6 hashes out the strategy for analysis and presents the data and simulated sets that will be used in the analysis.
- Chapter 7 demonstrates the implementation of the event selection processes.
- In Chapter 8 those events selected in Chapter 7 are analyzed.
- Chapter 9 presents a final discussion of the analyses presented in the thesis.

1.1 Review and Motivation

We assume that four-dimensional QCD can be modeled by the following five-dimensional action, written in the string frame:

$$\mathcal{S} = \frac{1}{16\pi G_5}\int d^5x\sqrt{-g}e^{-2\Phi}\left(R + 4\partial_M\Phi\partial^M\Phi - \mathrm{Tr}\left[|DX|^2 + \partial_M\mathcal{G}\partial^M\mathcal{G} + \frac{1}{2g_5^2}(F_A^2+F_V^2) + V_m(\Phi, X^2, \mathcal{G})\right]\right. \tag{1.1}$$

where Φ is the dilaton and the metric is pure AdS, $g_{MN} = z^{-2}\eta_{MN}$, with the AdS curvature defined to be unity. The constant $g_5^2 = 12\pi^2/N_c$, where N_c is the number of colors. The covariant derivative is defined as $D_M = \partial_M + i[V_M, X] - i\{A_M, X\}$. The scalar field, X, which is dual to the $\bar{q}q$ operator, obtains a z-dependent vacuum expectation value (VEV):

$$\langle X\rangle = \frac{\chi(z)}{2}I, \tag{1.2}$$

where I is the 2×2 identity matrix. The glueball field $\mathcal{G}$ similarly obtains a z-dependent VEV, $G(z)$. We examine the background dynamics of the fields

$$\mathcal{S} = \frac{1}{16\pi G_5}\int d^5x\sqrt{-g}e^{-2\Phi}\left(R + 4\partial_M\Phi\partial^M\Phi - \tfrac{1}{2}\partial_M\chi\partial^M\chi - \tfrac{1}{2}\partial_M G\partial^M G - V(\Phi,\chi,G)\right), \tag{1.3}$$

where $V = \mathrm{Tr}[V_m]$. The scalar fields Φ, χ, G are dimensionless.

It is easier to search for the background fields in the Einstein frame, where the vacuum action takes the canonical form

$$\mathcal{S}_E = \frac{1}{16\pi G_5}\int d^5x\sqrt{-\tilde{g}}\left(\tilde{R} - \tfrac{1}{2}\partial_M\phi\partial^M\phi - \tfrac{1}{2}\partial_M\chi\partial^M\chi - \tfrac{1}{2}\partial_M G\partial^M G - \tilde{V}(\phi,\chi)\right). \tag{1.4}$$

The tilde distinguishes the two frames, with $\tilde{V} = e^{4\Phi/3}V$, and the dilaton is rescaled for a canonical action $\phi = \sqrt{8/3}\Phi$. The string and Einstein frame metrics are related by the conformal transformation

$$g_{MN} = e^{2\phi/\sqrt{6}}\tilde{g}_{MN}. \tag{1.5}$$

Previous work showed how to construct a potential for a gravity-dilaton-chiral system without the glueball condensate. We examine the behavior assuming that the fields have power-law behavior, which is accurate in both the UV and IR limits, [**?**]. One of the equations of motion is independent of the choice of potential,

$$\dot{\chi}^2 = \frac{\sqrt{6}}{z^2}\frac{d}{dz}(z^2\dot{\phi}). \tag{1.6}$$

To obtain linear confinement, the dilaton should have quadratic behavior in the IR limit, $\phi(z) = \lambda z^2$. The chiral field should have have linear behavior, $\chi(z) = Az$, where A sets the large-n mass splitting between the axial-vector and vector mesons in the model. This constant mass-splitting at large n occurs because of the non-restoration of chiral symmetry [**?**]. Inserting this into (1.6), we find that the chiral field behaves as

$$\chi(z) = 6^{3/4}\sqrt{\lambda}z, \tag{1.7}$$

which removes one of the independent parameters of the model in [**?**]. Using the phenomenological value of λ, which determines the slope of the Regge trajectories, we find a mass splitting that is much too large.

Because this problem arises in the equation that is independent of the potential, this issue cannot be resolved by the choice of potential in models that do not consider the glueball condensate. Models that derive the field behavior using the superpotential method suffer from the same problem.

To resolve this problem, we consider the effects of the glueball condensate G on the background equations. This field must be linear in the IR for linear confinement, and go as $G \sim z^4$ in the UV to match the operator dimension in the AdS/CFT dictionary.

It is noted that the model proposed by Huang and Li [**?**, **?**] accurately models the non-restoration of chiral symmetry using a model with only two background fields, but their model differs from the work presented here in several respects. They place the meson fields and chiral dynamics in the open-string sector of the model. For linear confinement, this requires that the chiral field approach a constant in the IR, which necessitates a modified metric to obtain the correct chiral dynamics. Our model allows the metric to remain purely AdS in the string frame. Finally, they do not determine an explicit form of the potential, which is the central goal of this work.

1.2 Construction of Potential

Consider the action in the Einstein frame (1.4). To simplify the equations of motion, we use a transformed potential,

$$V = e^{-2\phi/\sqrt{6}}\tilde{V}. \tag{1.8}$$

It is noted that this is simply the potential in the string frame. We re-write the potential as

$$V = -12 + 4\sqrt{6}\phi + a_0\phi^2 + \frac{m_X^2}{2}\chi^2 + U. \tag{1.9}$$

Here U is more than quadratic in the fields. The AdS/CFT dictionary sets the mass for the fields according to the dimension of the dual operator,

$$m^2L^2 = \Delta(\Delta - 4). \tag{1.10}$$

The dimension of the $q\bar{q}$ operator is 3, so $m_X^2 = -3/L^2$. The dilaton mass is undetermined and is not connected to the dimension of the corresponding operator, as discussed in [**?**]. It is related to the parameter a_0 by $a_0 = \frac{1}{2}\left[(m_\phi L)^2 - 8\right]$. The potential should be an even function of χ.

The equations of motion can be written as

$$\dot{\chi}^2 + \dot{G}^2 = \frac{\sqrt{6}}{z^2}\frac{d}{dz}(z^2\dot{\phi}) \tag{1.11}$$

$$U = \tfrac{1}{2}\sqrt{6}z^2\ddot{\phi} - \tfrac{3}{2}(z\dot{\phi})^2 - 3\sqrt{6}z\dot{\phi} - 4\sqrt{6}\phi - a_0\phi^2 + \tfrac{3}{2}\chi^2 \tag{1.12}$$

$$\frac{\partial U}{\partial \phi} = 3z\dot{\phi} - 2a_0\phi \tag{1.13}$$

$$\frac{\partial U}{\partial \chi} = z^2\ddot{\chi} - 3z\dot{\chi}\left(1 + \frac{z\dot{\phi}}{\sqrt{6}}\right) + 3\chi \tag{1.14}$$

$$\frac{\partial U}{\partial G} = z^2\ddot{G} - 3z\dot{G}\left(1 + \frac{z\dot{\phi}}{\sqrt{6}}\right) \tag{1.15}$$

We assume that the potential has no explicit dependence on the coordinate z, so the equations 1.13-1.15 are not independent, and we can eliminate one.

1.2.1 IR Limit

The requirement of linear confinement requires a solution in the large z limit of the form

$$\phi = \lambda z^2 \tag{1.16}$$

$$\chi = Az \tag{1.17}$$

$$G = Bz. \tag{1.18}$$

Substitution into (1.11) gives

$$A^2 + B^2 = 6\sqrt{6}\lambda \tag{1.19}$$

The λ is fixed by the slope of the linear trajectory and A is fixed by the axial-vector – vector mass difference. It is useful to write these as

$$A = 6^{3/4}\sqrt{\lambda}\cos\theta$$

$$B = 6^{3/4}\sqrt{\lambda}\sin\theta, \tag{1.20}$$

where θ now becomes the parameter controlling the axial-vector – vector mass splitting. Inserting (1.18) into (1.12-1.15) suggests the following terms in our ansatz for the potential

$$U = a_1\phi\chi^2 + a_2\phi G^2 + a_3\chi^4 + a_4 G^4 + a_5\chi^2 G^2 + a_6 G^2\tanh(g\phi). \tag{1.21}$$

We see that there must be a G^2 term in the IR limit, but this is forbidden in the weak-field limit because the glueball condensate field is massless. To circumvent this, we propose the term $G^2\tanh(g\phi)$ with $g > 0$. In the weak field limit this goes to $g\phi G^2$, which is acceptable. The tanh is suggested by 1.8, and it suggests a rapid exponential transition from the weak field to the strong field limits that is supported by phenomenology. By substitution one finds the following constraints on the parameters:

$$U \to 6 + a_0 + 6\sqrt{6}\left(\cos^2\theta\, a_1 + \sin^2\theta\, a_2\right)$$

$$+6^3\left(\cos^4\theta\, a_3 + \sin^4\theta\, a_4 + \cos^2\theta\sin^2\theta\, a_5\right) = 0 \tag{1.22}$$

$$\frac{\partial U}{\partial\chi} \to 2a_1 + 24\sqrt{6}\cos^2\theta\, a_3 + 12\sqrt{6}\sin^2\theta\, a_5 + \sqrt{6} = 0 \tag{1.23}$$

$$\frac{\partial U}{\partial G} \to 2a_2 + 24\sqrt{6}\sin^2\theta\, a_4 + 12\sqrt{6}\cos^2\theta\, a_5 + \sqrt{6} = 0 \tag{1.24}$$

$$\frac{\partial U}{\partial G} \to a_6 = -\tfrac{3}{2} \tag{1.25}$$

We have chosen to exclude (1.13) because it is not independent. The parameter a_6 is determined, and the others will be determined by an examination of the UV limit.

1.2.2 UV Limit

Next we look for a solution in the small z limit. The AdS/CFT dictionary dictates that the leading-order UV behavior of the chiral and glueball condensate fields is determined by their dimension. Note also that we are working in the chiral limit where the quark mass is zero. We start by examining only the leading-order terms

$$\chi = \Sigma_0 z^3 \tag{1.26}$$

$$G = G_0 z^4. \tag{1.27}$$

Substitution into (1.11) and imposing the boundary condition $\phi(0) = 0$ gives

$$\phi = \frac{\sqrt{6}}{28}\Sigma_0^2 z^6 + \frac{\sqrt{6}}{27}G_0^2 z^8 \tag{1.28}$$

Using only this leading-order behavior in (1.12-1.15), the system of equations is inconsistent, as there are more equations from matching powers of z than unknown parameters.

To solve this problem, try adding a term $\Sigma_n z^n$ to χ. Substituting into (1.11) and keeping only the lowest-order cross-term we find the additional term in ϕ

$$\Delta\phi = \frac{\sqrt{6}n\Sigma_0\Sigma_n}{(n+4)(n+3)}z^{n+3} \tag{1.29}$$

From (1.12) we find that

$$U = -\tfrac{3}{2}(z\dot{\phi})^2 - a_0\phi^2 + 3\frac{n^3 - 13n + 12}{(n+4)(n+3)}\Sigma_0\Sigma_n z^{n+3} \tag{1.30}$$

Since the ϕ^2 terms start out as z^{12}, z^{14}, z^{16}, and so do the terms in the potential, the n can only take the values 9, 11, etc. This term contributes only to the equation for $\partial U/\partial\chi$.

$$\frac{\partial U}{\partial \chi} = -9\Sigma_0\left(\frac{3}{14}\Sigma_0^2 + \frac{8}{27}G_0^2 z^2\right)z^9 + (n-3)(n-1)\Sigma_n z^n \tag{1.31}$$

By power counting both $n = 9$ and $n = 11$ can contribute.

There could also be higher order terms in G such as $G_m z^m$. This leads to the additional term in ϕ

$$\Delta\phi = \frac{8mG_0G_m}{\sqrt{6}(m+5)(m+4)}z^{m+4} \tag{1.32}$$

It contributes to the equation for $\partial U/\partial G$ as

$$\frac{\partial U}{\partial G} = -12G_0\left(\frac{3}{14}\Sigma_0^2 + \frac{8}{27}G_0^2 z^2\right)z^{10} + m(m-4)G_n z^m \tag{1.33}$$

The choice $m = 8$ is not possible as there is no term of the same order to balance it. Terms with $m = 10$ and $m = 12$ are possible. These new terms cannot affect the equation for $\partial U/\partial\phi$ nor can they contribute to the equation for $\partial U/\partial\chi$. Considering higher order terms in both χ and G leads to

$$U = -\tfrac{3}{2}(z\dot{\phi})^2 - a_0\phi^2 + 3\frac{n^3 - 13n + 12}{(n+4)(n+3)}\Sigma_0\Sigma_n z^{n+3} + \frac{4m(m-4)}{m+4}G_0G_m z^{m+4} \tag{1.34}$$

The appearance of these terms can be understood by writing the following schematic expansions.

$$\chi \sim \Sigma_0 z^3 + \Sigma_0^3 z^9 + G_0^2\Sigma_0 z^{11} + \cdots$$
$$G \sim G_0 z^4 + \Sigma_0^2 G_0 z^{10} + G_0^3 z^{12} + \cdots$$

That is, χ is an odd function of Σ_0 and G is an odd function of G_0. These are the symmetries in the equations of motion. They also follow the spirit of the AdS/CFT correspondence in terms of the dimensionality of the operators and the powers of z.

Including now $m = 10$ and 12, and $n = 9$ and 11, we have the following set of equations in the small z limit:

$$\begin{aligned} U_{\rm LHS} &= 3\Sigma_0^4 z^{12}\left[4\frac{\Sigma_9}{\Sigma_0^3} - \frac{(54+a_0)}{2^3\cdot 7^2}\right] \\ &+ \frac{1}{7}\Sigma_0^2 G_0^2 z^{14}\left[120\frac{G_{10}}{\Sigma_0^2 G_0} + 120\frac{\Sigma_{11}}{\Sigma_0 G_0^2} - \frac{(72+a_0)}{9}\right] \\ &+ 2G_0^4 z^{16}\left[12\frac{G_{12}}{G_0^3} - \frac{(96+a_0)}{3^5}\right] \end{aligned} \tag{1.35}$$

$$\begin{aligned} U_{\rm RHS} &= \Sigma_0^4 z^{12}\left[\frac{\sqrt{6}}{28}a_1 + a_3\right] \\ &+ \Sigma_0^2 G_0^2 z^{14}\left[\frac{\sqrt{6}}{27}a_1 + \frac{\sqrt{6}}{28}(a_2 + g a_6) + a_5\right] \\ &+ G_0^4 z^{16}\left[\frac{\sqrt{6}}{27}(a_2 + g a_6) + a_4\right] \end{aligned} \tag{1.36}$$

$$\left(\frac{\partial U}{\partial\chi}\right)_{\rm LHS} = 3\Sigma_0^3 z^9\left[-\frac{9}{14} + 16\frac{\Sigma_9}{\Sigma_0^3}\right] + 8\Sigma_0 G_0^2 z^{11}\left[-\frac{1}{3} + 10\frac{\Sigma_{11}}{\Sigma_0 G_0^2}\right] \tag{1.37}$$

$$\left(\frac{\partial U}{\partial\chi}\right)_{\rm RHS} = \Sigma_0^3 z^9\left[\frac{\sqrt{6}}{14}a_1 + 4a_3\right] + \Sigma_0 G_0^2 z^{11}\left[\frac{2\sqrt{6}}{27}a_1 + 2a_5\right] \tag{1.38}$$

$$\left(\frac{\partial U}{\partial G}\right)_{\rm LHS} = 6\Sigma_0^2 G_0 z^{10}\left[-\frac{3}{7}+10\frac{G_{10}}{\Sigma_0^2 G_0}\right]+32G_0^3 z^{12}\left[-\frac{1}{9}+3\frac{G_{12}}{G_0^3}\right] \quad (1.39)$$

$$\left(\frac{\partial U}{\partial G}\right)_{\rm RHS} = \Sigma_0^2 G_0 z^{10}\left[\frac{\sqrt{6}}{14}(a_2+ga_6)+2a_5\right] \quad (1.40)$$

$$+ \; G_0^3 z^{12}\left[\frac{2\sqrt{6}}{27}(a_2+ga_6)+4a_4\right] \quad (1.41)$$

Altogether, from both the UV and IR limits, there are ten independent equations for the twelve parameters $a_0 - a_6$, Σ_9, Σ_{11}, G_{10}, G_{12}, and g. We take g as the free parameter to use as the rate of transition from small z to large z. The parameters in the potential are found to be

$$a_0 = \frac{3}{2}\frac{1}{6+\sin^2\theta}\left[120+62\sin^2\theta+63\sqrt{6}g\sin^2\theta\right] \quad (1.42)$$

$$a_1 = -\frac{3\sqrt{6}}{4}\frac{1}{6+\sin^2\theta}\left[12+8\sin^2\theta+9\sqrt{6}g\sin^2\theta\right] \quad (1.43)$$

$$a_2 = -\frac{\sqrt{6}}{4}\frac{1}{6+\sin^2\theta}\left[32+24\sin^2\theta+3\sqrt{6}g(9\sin^2\theta-2)\right] \quad (1.44)$$

$$2a_3\cos^2\theta+a_5\sin^2\theta = \frac{1}{24}\frac{1}{6+\sin^2\theta}\left[24+22\sin^2\theta+27\sqrt{6}g\sin^2\theta\right] \quad (1.45)$$

$$2a_4\sin^2\theta+a_5\cos^2\theta = \frac{1}{24}\frac{1}{6+\sin^2\theta}\left[20+22\sin^2\theta+3\sqrt{6}g(9\sin^2\theta-2)\right] \quad (1.46)$$

$$a_6 = -\frac{3}{2} \quad (1.47)$$

The coefficients a_0, a_1, a_2 and a_6 are determined, while there are two equations for the three coefficients a_3, a_4 and a_5. That leaves a_5 as a free parameter, to be fit numerically, along with g, θ, G_0, Σ, and λ.

1.3 Numerical Solution

Using the above potential, we seek a numerical solution that simultaneously satisfies the UV and IR limits. We use equations (1.11, 1.14, 1.15), which allows for an additional term in the potential, ΔU, such that

$$\frac{\partial}{\partial\chi}\Delta U = \frac{\partial}{\partial G}\Delta U = 0, \quad (1.48)$$

which will be determined from the numerical solution.

The differential equations represent a stiff system, and treatment of the problem as an initial value problem leads to numerical instabilities. We treat it instead as a boundary value problem, using Dirichlet boundary conditions at both boundaries. A relaxation method is used in combination with input approximations for the background fields, which are then iterated to find a stable solution to the system with the given boundary conditions. Because the system is nonlinear, the solution found is not guaranteed to be unique.

The IR boundary is chosen to be sufficiently large to capture the infrared behavior and to give accurate Regge behavior large-n radial excitations of the mesons. The UV boundary should approach zero, but it cannot reach zero because of the singularity in the equations of motion. This becomes a problem because equation (1.11) allows constant and divergent terms

$$\Delta\phi(z) = c_1 + c_2 z^{-1}. \tag{1.49}$$

Symbolically, these terms can be set to zero by enforcing the Dirichlet boundary condition $\phi(0) = 0$, but this is impossible to enforce numerically. Creative choice of UV boundary conditions can eliminate one, but not both of these unwanted terms without affecting the chiral and glueball fields. The behavior of the numerical solutions suggests that the desired UV behavior is an unstable solution to the equations, and therefore difficult or impossible to find with this iterative method.

As an alternative to direct solution, we parameterize the fields as follows:

$$\Psi(z) = \psi(z)_{UV} f(z) + \psi(z)_{IR} \left(1 - f(z)\right), \tag{1.50}$$

where $f(z)$ is some function that transitions smoothly from 1 at small values of z to 0 at large z, and $\psi(z)_{xx}$ represents the known UV and IR limits of the fields ϕ, χ, and G. The switching functions f need not be the same for each field. We choose

$$f_\phi(z) = e^{-(\beta_1 z)^{10}} \tag{1.51}$$

$$f_\chi(z) = e^{-(\beta_2 z)^4} \tag{1.52}$$

$$f_G(z) = e^{-(\beta_3 z)^5}. \tag{1.53}$$

The powers of the exponential are chosen to be greater than the known power-law behavior of the fields in the UV limit, so as to not interfere with this behavior. The β_i will be set by numerical fitting.

The chiral condensate Σ is set using the Gell-Mann–Oakes–Renner relation:

$$(m_u + m_d)\Sigma = f_\pi^2 m_\pi^2. \tag{1.54}$$

Using $m_\pi = 139.6$ MeV, $f_\pi = 92$ MeV, and $m_u + m_d = 7.0$ MeV yields a value of $\Sigma = (286\,\mathrm{MeV})^3$.

In all, we have eight parameters to be set numerically. The first constraint is to obtain the best global visual fit to the meson spectrum. We do not simply do a chi-squared fitting to the experimental data because the measurement error for the ground state ρ meson is so much smaller than for the others that this would effectively act as the only constraint. Secondly, we seek to minimize the error in the finite-difference approximations to equations 1.11, 1.14, and 1.15.

Three of the parameters are most phenomenologically relevant: λ, which controls the slope of the meson spectra in the large-n limit; θ, which controls the mass splitting between the a_1 and ρ mesons, and β_2, which controls the location of the "bend" in the a_1 spectrum. For each set of these parameters, the other parameters are set by a routine that minimizes the error in the equations of motion. The parameters found are shown in Table 1.1.

The background fields that are obtained from this analysis are shown in Figures 1.1-1.3. The asymptotic power-law behavior of the fields is evident in the linear portions of the log-log scale plots shown. The "transition" behavior is most evident in the dilaton because of the large value of β_1, which controls the value of z at which the field transitions from the UV limit to the IR limit.

We now analyze the "extra" term in the potential, ΔU. We obtain this term numerically by subtracting the right-hand side of 1.12 from its left-hand side. This term can be approximated numerically as a function of the dilaton field,

$$\Delta U\left(\Phi\right) = \alpha_1 \Phi^2 e^{-(\Phi-\gamma 1)^2/\delta 1} + \alpha_2 \Phi^2 e^{-(\Phi-\gamma_2)^2/\delta_2}. \tag{1.55}$$

The best-fit values for these parameters are shown in Table 1.3.

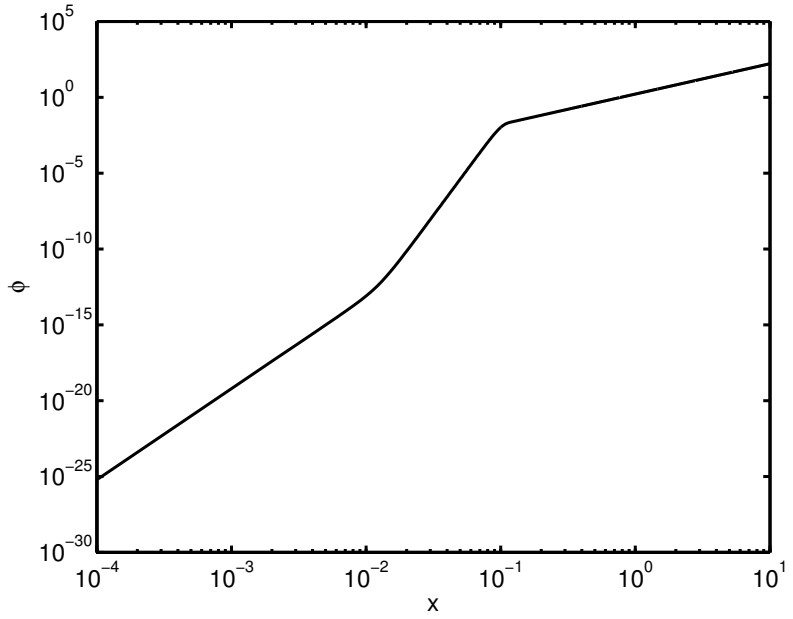

Figure 1.1: A plot of the dilaton field Φ generated by the parameterization (1.52). The UV and IR asymptotic behavior is apparent. The coordinate x is a dimensionless re-scaling of the conformal coordinate, $x = \sqrt{\lambda} z$.

$\lambda^{1/2}$	304 MeV	β_1	3.04 GeV
$G_0^{1/4}$	552 MeV	β_2	274 MeV
θ	1.44	β_3	558 MeV
g	3.20	a_5	1.63

Table 1.1: Best fit parameters for the phenomenological model. The parameters λ, θ, and β_2 are chosen for the best visual fit to the ρ and a_1 data, with the rest set by minimizing the error in the equations of motion (1.11), (1.14-1.15).

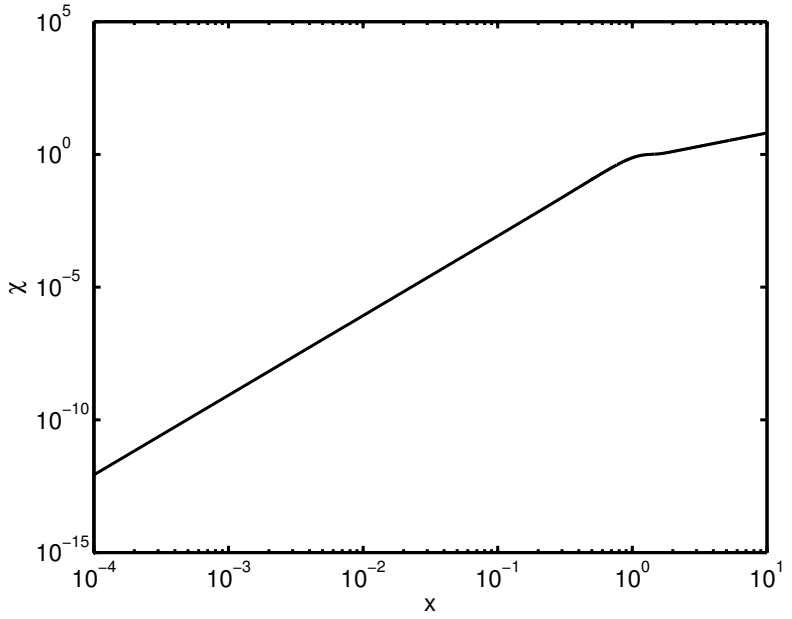

Figure 1.2: A plot of the chiral field χ generated by the parameterization (1.53). The UV and IR asymptotic behavior is apparent, with a rapid transition between them. The coordinate x is a dimensionless re-scaling of the conformal coordinate, $x = \sqrt{\lambda}z$.

α_1	-304.3 $\pm$ 5 $\times 10^{-1}$
γ_1	0.07086 $\pm$ 4 $\times 10^{-3}$
δ_1	0.09699 $\pm$ 1.3 $\times 10^{-3}$
α_2	0.2671 $\pm$ 6.4 $\times 10^{-3}$
γ_2	2.213 $\pm$ 4 $\times 10^{-2}$
δ_2	1.471 $\pm$ 9 $\times 10^{-2}$

Table 1.2: The dimensionless parameters for the fitting to ΔU

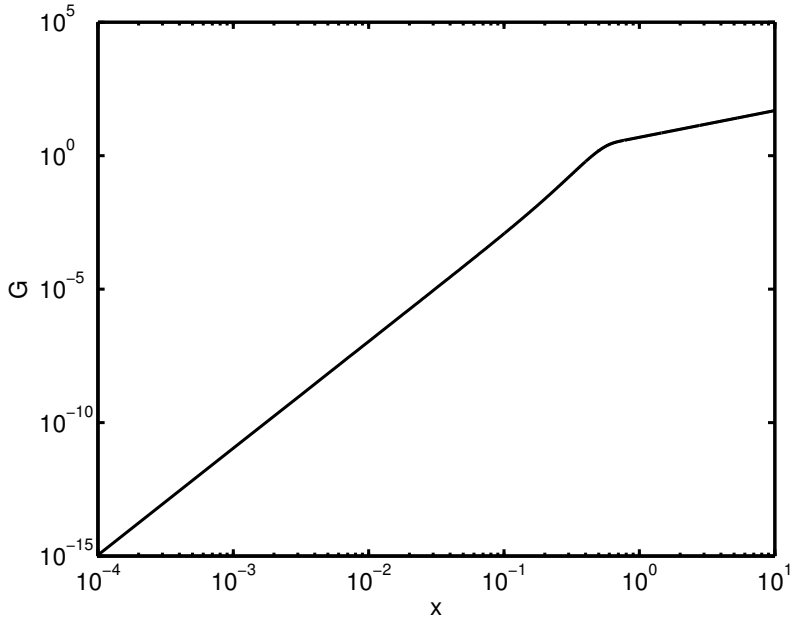

Figure 1.3: A plot of the glueball field G generated by the parameterization (1.53). The UV and IR asymptotic behavior is apparent, with a rapid transition between them. The coordinate x is a dimensionless re-scaling of the conformal coordinate, $x = \sqrt{\lambda}z$.

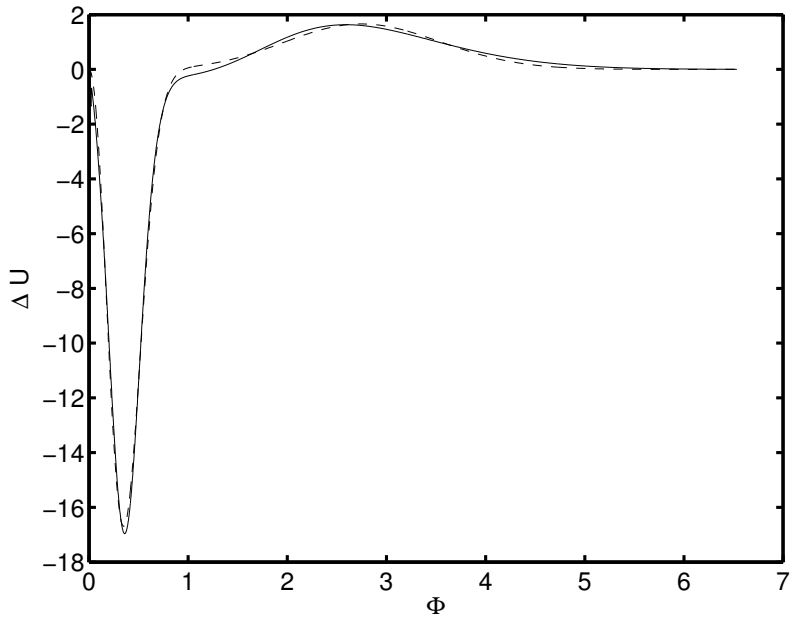

Figure 1.4: Plot of the "extra" term in the potential, $\Delta U(\phi)$. The solid line represents the numerical result, while the dashed line is the fitting of (1.55) using the parameters of Table 1.3.

Chapter 2

Conclusion and Discussion

Appendix A

Glossary and Acronyms